Approaching Unit Visibility for Control of a Superconducting Qubit with Dispersive Readout

A. Wallraff, D. I. Schuster, A. Blais, L. Frunzio, J. Majer, M. H. Devoret, S. M. Girvin, and R. J. Schoelkopf

Departments of Applied Physics and Physics, Yale University, New Haven, Connecticut 06520, USA

(Received 27 February 2005; published 1 August 2005)

In a Rabi oscillation experiment with a superconducting qubit we show that a visibility in the qubit excited state population of more than 95% can be attained. We perform a dispersive measurement of the qubit state by coupling the qubit nonresonantly to a transmission line resonator and probing the resonator transmission spectrum. The measurement process is well characterized and quantitatively understood. In a measurement of Ramsey fringes, the qubit coherence time is larger than 500 ns.

DOI: 10.1103/PhysRevLett.95.060501 PACS numbers: 03.67.Pp, 42.50.Pq, 85.35.Gv

One of the most promising solid-state architectures for the realization of a quantum information processor [1] is based on superconducting electrical circuits [2]. A variety of such circuits acting as qubits [1], the basic carriers of quantum information in a quantum computer, have been created and their coherent control has been demonstrated [3–8]. Recent experiments have realized controlled coupling between different qubits [9–13] and also first two-qubit quantum logic gates [14].

An outstanding question for superconducting qubits, and in fact for all solid-state implementations of quantum information processors, is whether the qubits are sufficiently well isolated to allow long coherence times and high-fidelity preparation and control of their quantum states. This question is complicated by inevitable imperfections in the measurement. A canonical example is a Rabi oscillation experiment, where the experimenter records the oscillations of a meter's response as a function of pulse length to infer the qubit's excited state population immediately after the pulse. The measurement contrast (e.g., the amplitude of the meter's measured swing relative to its maximum value) is reduced in general by both errors in the qubit preparation and readout, and sets a lower limit on the visibility of oscillations in the qubit population. Most experiments with superconducting qubits to date have reported only the measurement contrast, implying only a lower limit on the visibility in the range of 10%–50% [3–8,14].

A full understanding of the measurement process is required to extract the qubit population from the meter's output. The qubit control is then characterized by the visibility, defined as the maximum qubit population difference observed in a Rabi oscillation or Ramsey fringe experiment. It is essential to demonstrate that a qubit can be controlled without inducing undesired leakage to other qubit states or entanglement with the environment. Some experiments [15] observe a substantial reduction of the visibility due to entanglement with spurious environmental fluctuators [16]. In the few experiments in which the contrast has been characterized, it was close to the expected value [17,18], which implies that high visibility should be achievable with superconducting qubits.

In this Letter, we report results on time-domain control of the quantum state of a superconducting qubit, where the qubit state is determined using a dispersive microwave measurement in a circuit quantum electrodynamics (QED) architecture [19]. This novel technique has shown good agreement with predictions in steady-state experiments [20]. Here, we observe the measurement response, both during and after qubit state manipulation, which is in quantitative agreement with the theoretical model of the system, allowing us to separate the contributions of the qubit and the readout to the observed contrast. The observed contrast of 85% and a visibility of greater than 95% for Rabi oscillations demonstrates that high accuracy control is possible in superconducting qubits.

In our circuit QED architecture [19], a Cooper pair box [21], acting as a two level system with ground $|\downarrow\rangle$ and excited states $|\uparrow\rangle$ and level separation $E_a = \hbar\omega_a = \sqrt{E_{el}^2 + E_J^2}$ is coupled capacitively to a single mode of the electromagnetic field of a transmission line resonator with resonance frequency ω_r; see Fig. 1(a). As demonstrated for this system, the electrostatic energy E_{el} and the Josephson energy E_J of the split Cooper pair box can be controlled *in situ* by a gate voltage V_g and magnetic flux Φ [20,22]; see Fig. 1(a). In the resonant ($\omega_a = \omega_r$) strong coupling regime a single excitation is exchanged coherently between the Cooper pair box and the resonator at a rate g/π, also called the vacuum Rabi frequency [22]. In the nonresonant regime ($|\Delta| = |\omega_a - \omega_r| > g$) the capacitive interaction gives rise to a dispersive shift $(g^2/\Delta)\sigma_z$ in the resonance frequency of the cavity which depends on the qubit state σ_z, the coupling g, and the detuning Δ [19,20]. We have suggested that this shift in resonance frequency can be used to perform a quantum nondemolition (QND) measurement of the qubit state [19]. With this technique we have recently measured the ground state response and the excitation spectrum of a Cooper pair box [20,22].

In the experiments presented here, we coherently control the quantum state of a Cooper pair box in the resonator by applying microwave pulses of frequency ω_s, which are resonant or nearly resonant with the qubit transition frequency $\omega_a/2\pi \approx 4.3$ GHz, to the input port C_{in} of the resonator; see Fig. 1(a). Even though ω_s is strongly de-

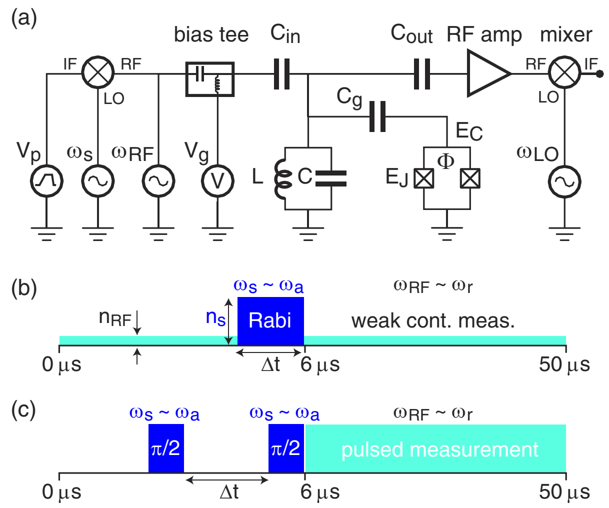

FIG. 1 (color online). (a) Simplified circuit diagram of measurement setup. A Cooper pair box with charging energy E_C and Josephson energy E_J is coupled through capacitor C_g to a transmission line resonator, modeled as parallel combination of an inductor L and a capacitor C. Its state is determined in a phase sensitive heterodyne measurement of a microwave transmitted at frequency ω_{RF} through the circuit, amplified and mixed with a local oscillator at frequency ω_{LO}. The Cooper pair box level separation is controlled by the gate voltage V_g and flux Φ. Its state is coherently manipulated using microwaves at frequency ω_s with pulse shapes determined by V_p [8]. (b) Measurement sequence for Rabi oscillations with Rabi pulse length Δt, pulse frequency ω_s, and amplitude $\propto \sqrt{n_s}$ with continuous measurement at frequency ω_{RF} and amplitude $\propto \sqrt{n_{RF}}$. (c) Sequence for Ramsey fringe experiment with two $\pi/2$ pulses at ω_s separated by a delay Δt and followed by a pulsed measurement.

tuned from the resonator frequency ω_r, the resonator can be populated with n_s drive photons which induce Rabi oscillations in the qubit at a frequency of $\nu_{Rabi} = \sqrt{n_s} g/\pi$. Simultaneously, we perform a continuous dispersive measurement of the qubit state by determining both the phase and the amplitude of a coherent microwave beam transmitted through the resonator at frequency ω_{RF} which is resonant or nearly resonant with the resonator frequency $\omega_r/2\pi \approx 5.4$ GHz [19,22]. The phase shift $\phi = \tan^{-1}(2g^2/\kappa\Delta)\sigma_z$ is the response of our meter from which we determine the qubit population. For the measurement, we chose a resonator that has a quality factor of $Q \sim 0.7 \times 10^4$ corresponding to a photon decay rate of $\kappa/2\pi = 0.73$ MHz. The resonator is populated with $n \sim 1$ measurement photons on average, where n is calibrated using the ac-Stark shift [20]. All experiments are performed in a dilution refrigerator at a temperature of 20 mK. The charging energy of the box is $E_C = e^2/2C \approx h\ 5.2$ GHz. Details on the device fabrication can be found in Ref. [23].

We initially determine the maximum swing of the meter in a calibration measurement by first maximizing the detuning Δ to minimize the interaction ($g^2/\Delta \to 0$) which defines $\phi = 0$. We prepare the Cooper pair box in the ground state $|\downarrow\rangle$ by relaxation, the thermal population of excited states being negligible. The box is biased at charge degeneracy ($E_{el} = 0$), where its energy is to first-order insensitive to charge noise [4]. Using flux bias, the detuning is adjusted to $\Delta/2\pi \approx -1.1$ GHz corresponding to a maximum in the Josephson coupling energy of $E_J/h \approx 4.3$ GHz $< \omega_r/2\pi$. In this case we measure a minimum meter response of $\phi_{|\downarrow\rangle} = -35.3$ deg corresponding to a coupling strength of $g/2\pi = 17$ MHz. Saturating the qubit transition by applying a long microwave pulse which incoherently mixes the ground and excited states such that the occupation probabilities are $P_{|\downarrow\rangle} = P_{|\uparrow\rangle} = 1/2$, the measured phase shift is found to be $\phi = 0$, as expected [20]. From these measurements, the predicted phase shift induced by a fully polarized qubit ($P_{|\uparrow\rangle} = 1$) would be $\phi_{|\uparrow\rangle} = 35.3$ deg. Thus, the maximum swing of the meter is bounded by $\phi_{|\uparrow\rangle} - \phi_{|\downarrow\rangle}$.

In our measurement of Rabi oscillations, a short microwave pulse of length Δt is applied to the qubit in its ground state with a repetition rate of 20 kHz while the measurement response ϕ is continuously monitored and digitally averaged 5×10^4 times; see Fig. 1(b). The signal to noise ratio (SNR) in the averaged value of ϕ in an integration time of 100 ns is approximately 25, see Fig. 2, corresponding to a SNR of 0.1 in a single shot. For the present setup the single shot readout fidelity for the qubit state integrated over the relaxation time ($T_1 \sim 7$ μs) is approximately 30% [24]. Either a readout amplifier with lower noise temperature or a larger signal power would potentially allow a high-fidelity single shot measurement of the qubit state in this setup.

The time dependence of the averaged value of ϕ in response to a π pulse of duration $\Delta t \sim 16$ ns applied to the qubit is shown in Fig. 2(a). Before the start of the pulse the measured phase shift is $\phi_{|\downarrow\rangle} \approx -35.3$ deg corresponding to the qubit being in the ground state. Because of the state change of the qubit induced by the pulse, the resonator frequency is pulled by $2g^2/\Delta$ and, thus, the measured phase shift is seen to rise exponentially towards $\phi_{|\uparrow\rangle}$ with the resonator amplitude response time $2/\kappa \approx 400$ ns, i.e., twice the photon life time. After the π pulse, the qubit excited state decays exponentially with its energy relaxation time $T_1 \sim 7.3$ μs, as extracted from the decay in the measured phase shift; see Fig. 2(a). As a result, the maximum measured response ϕ_{max} does not reach the full value of $\phi_{|\uparrow\rangle}$. In general, the measurement contrast $C = (\phi_{max} - \phi_{min})/(\phi_{|\uparrow\rangle} - \phi_{|\downarrow\rangle})$ will be reduced in any qubit readout for which the qubit lifetime is not infinitely longer than the measurement response time. Additionally, in non-QND measurements the contrast is reduced even further due to mixing of the qubit states induced by the interaction with the measurement apparatus. In our QND measurement presented here, the qubit lifetime is about 15 times the response time of the measurement, allowing us to reach a high maximum contrast of $C \sim 85\%$ in the bare measurement response ϕ.

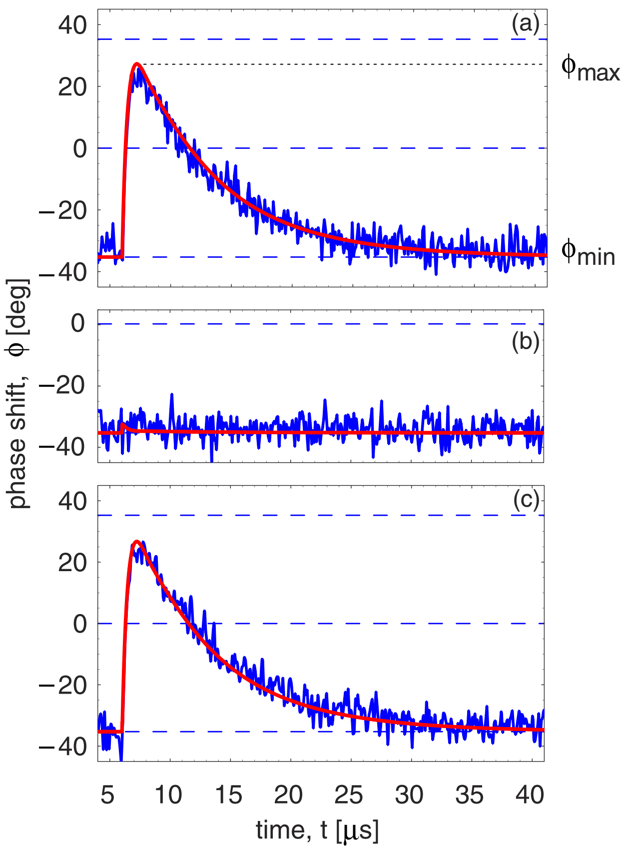

FIG. 2 (color online). Measurement response ϕ (blue lines) and theoretical prediction (red lines) vs time. At $t = 6$ μs (a) a π pulse, (b) a 2π pulse, and (c) a 3π pulse is applied to the qubit. In each panel the dashed lines correspond to the expected measurement response in the ground state $\phi_{|\downarrow\rangle}$, in the saturated state $\phi = 0$, and in the excited state $\phi_{|\uparrow\rangle}$.

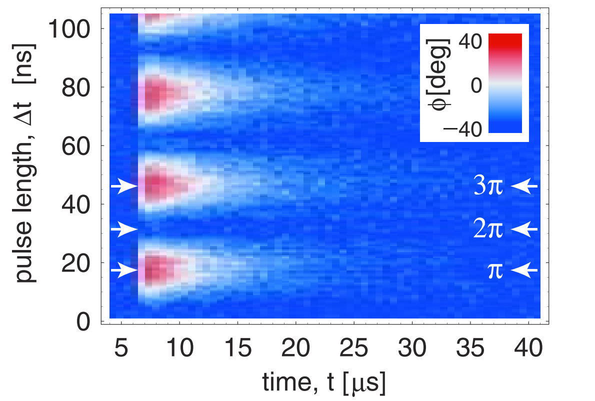

FIG. 3 (color online). Color density plot of phase shift ϕ (see inset for scale) versus measurement time t and Rabi pulse length Δt. Data shown in Fig. 2 are slices through this data set at the indicated pulse lengths.

In Figs. 2(b) and 2(c), the measured response ϕ of the meter to a 2π and a 3π pulse acting on the qubit is shown. As expected, no phase shift is observable for the 2π pulse since the response time of the resonator is much longer than the duration $\Delta t = 32$ ns of the pulse. In agreement with the expectations for this QND scheme, the measurement does not excite the qubit, i.e., $\phi_{\min} = \phi_{\max} = \phi_{|\downarrow\rangle}$. The response to the 3π pulse is virtually indistinguishable from the one to the π pulse, as expected for the long coherence and energy relaxation times of the qubit. In the 2D density plot Fig. 3, Rabi oscillations are clearly observed in the phase shift acquired versus measurement time t and Rabi pulse length Δt.

The observed measurement response ϕ is in excellent agreement with theoretical predictions, see red lines in Fig. 2, demonstrating a good understanding of the measurement process. The temporal response $\phi(t) = \arg\{i\langle a(t)\rangle\}$ of the cavity field a is calculated by deriving and solving Bloch-type equations of motion for the cavity and qubit operators [25] using the Jaynes-Cummings Hamiltonian in the dispersive regime [19,20] as the starting point. A semiclassical factorization approximation is done to truncate the resulting infinite set of equations to a finite set (e.g., $\langle a^\dagger a \sigma_z\rangle \sim \langle a^\dagger a\rangle\langle\sigma_z\rangle$; all lower order products are kept). This amounts to neglecting higher order correlations between qubit and field which is a valid approximation in the present experiment. The calculations accurately model the exponential rise in the observed phase shift on the time scale of the resonator response time due to a state change of the qubit. They also accurately capture the reduced maximum response $\phi_{\max}$ due to the exponential decay of the qubit. Overall, excellent agreement in the temporal response of the measurement is found over the full range of qubit and measurement time scales with no adjustable parameters; see Fig. 2.

The visibility of the excited state population $P_{|\uparrow\rangle}$ in the Rabi oscillations is extracted from the time dependent measurement response ϕ for each Rabi pulse length Δt. We find $P_{|\uparrow\rangle}$ by calculating the normalized dot product between the measured response ϕ and the predicted response taking into account the systematics of the measurement. This amounts to comparing the area under a measured response curve to the theoretically predicted area; see Fig. 2. The averaged response of all measurements taken over a window in time extending from the start of the Rabi pulse out to several qubit decay times T_1 is used to extract $P_{|\uparrow\rangle}$. This maximizes the signal to noise ratio in the extracted Rabi oscillations.

The extracted qubit population $P_{|\uparrow\rangle}$ is plotted versus Δt in Fig. 4(a). We observe a visibility of $95 \pm 6\%$ in the Rabi oscillations with error margins determined from the residuals of the experimental $P_{|\uparrow\rangle}$ with respect to the predicted values. Thus, in a measurement of Rabi oscillations in a superconducting qubit, a visibility in the population of the qubit excited state that approaches unity is observed for the first time. Moreover, the decay in the Rabi oscillation amplitude out to pulse lengths of 100 ns is very small and consistent with the long T_1 and T_2 times of this charge

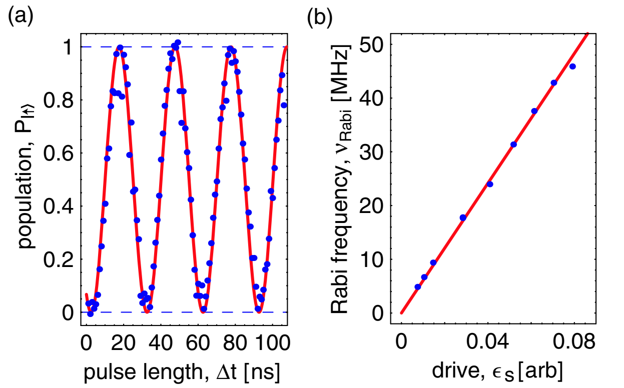

FIG. 4 (color online). (a) Rabi oscillations in the qubit population $P_{|\uparrow\rangle}$ vs Rabi pulse length Δt (blue dots) and fit with unit visibility (red line). (b) Measured Rabi frequency ν_{Rabi} vs pulse amplitude ϵ_s (blue dots) and linear fit.

qubit; see Fig. 4(a) and Ramsey experiment discussed below. We have also verified the expected linear scaling of the Rabi frequency ν_{Rabi} with the pulse amplitude $\epsilon_s \propto \sqrt{n_s}$; see Fig. 4(b).

We have determined the coherence time of the Cooper pair box from a Ramsey fringe experiment at charge degeneracy using $\pi/2$ pulses of 20 ns duration; see Fig. 1(c). To avoid dephasing induced by a weak continuous measurement beam [20] we switch on the measurement beam only after the end of the second $\pi/2$ pulse. The resulting Ramsey fringes oscillating at the detuning frequency $\delta_{a,s} = \omega_a - \omega_s \sim 6$ MHz decay with a long coherence time of $T_2 \sim 500$ ns; see Fig. 5(a). The corresponding qubit phase quality factor of $Q_\varphi = T_2\omega_a/2 \sim 6500$ is

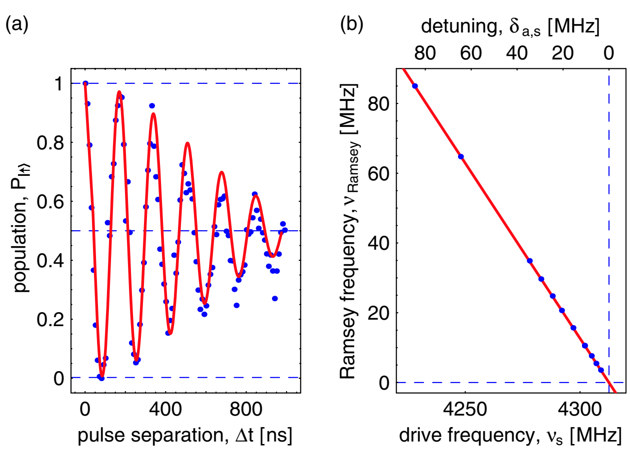

FIG. 5 (color online). (a) Measured Ramsey fringes (blue dots) observed in the qubit population $P_{|\uparrow\rangle}$ vs pulse separation Δt using the pulse sequence shown in Fig. 1(b) and fit of data to sinusoid with Gaussian envelope (red line). (b) Measured dependence of Ramsey frequency ν_{Ramsey} on detuning $\delta_{a,s}$ of drive frequency (blue dots) and linear fit (red line).

similar to the best values measured so far in qubits biased at an optimal point [4]. The Ramsey frequency is shown to depend linearly on the detuning $\delta_{a,s}$, as expected; see Fig. 5(b). We note that a measurement of the Ramsey frequency is an accurate time resolved method to determine the qubit transition frequency $\omega_a = \omega_s + 2\pi\nu_{\mathrm{Ramsey}}$.

In conclusion, performing Rabi and Ramsey experiments we have observed high visibility in the oscillations of state population of a superconducting qubit. The temporal response and the backaction of the readout are quantitatively understood and well characterized. Our charge qubit, which is embedded in a well-controlled electromagnetic environment, has T_1 and T_2 times among the longest realized so far in superconducting systems. The simplicity and level of control possible in this circuit QED architecture makes it an attractive candidate for superconducting quantum computation.

We thank Jay Gambetta for discussions. This work was supported in part by NSA and ARDA under ARO Contract No. DAAD19-02-1-0045, and the NSF under Grants No. ITR-0325580 and No. DMR-0342157, the David and Lucile Packard Foundation, the W. M. Keck Foundation, and the NSERC of Canada.

[1] M. A. Nielsen and I. L. Chuang, *Quantum Computation and Quantum Information* (Cambridge University Press, Cambridge, 2000).
[2] M. H. Devoret, A. Wallraff, and J. M. Martinis, cond-mat/0411174.
[3] Y. Nakamura, Y. A. Pashkin, and J. S. Tsai, Nature (London) **398**, 786 (1999).
[4] D. Vion *et al.*, Science **296**, 886 (2002).
[5] J. M. Martinis *et al.*, Phys. Rev. Lett. **89**, 117901 (2002).
[6] Y. Yu *et al.*, Science **296**, 889 (2002).
[7] I. Chiorescu *et al.*, Science **299**, 1869 (2003).
[8] E. Collin *et al.*, Phys. Rev. Lett. **93**, 157005 (2004).
[9] A. J. Berkley *et al.*, Science **300**, 1548 (2003).
[10] Y. A. Pashkin *et al.*, Nature (London) **421**, 823 (2003).
[11] J. B. Majer *et al.*, Phys. Rev. Lett. **94**, 090501 (2005).
[12] I. Chiorescu *et al.*, Nature (London) **431**, 159 (2004).
[13] R. McDermott *et al.*, Science **307**, 1299 (2005).
[14] T. Yamamoto *et al.*, Nature (London) **425**, 941 (2003).
[15] R. Simmonds *et al.*, Phys. Rev. Lett. **93**, 077003 (2004).
[16] F. Meier and D. Loss, Phys. Rev. B **71**, 094519 (2005).
[17] T. Duty *et al.*, Phys. Rev. B **69**, 140503 (2004).
[18] O. Astafiev *et al.*, Phys. Rev. B **69**, 180507 (2004).
[19] A. Blais *et al.*, Phys. Rev. A **69**, 062320 (2004).
[20] D. I. Schuster *et al.*, Phys. Rev. Lett. **94**, 123602 (2005).
[21] V. Bouchiat *et al.*, Phys. Scr. **t76**, 165 (1998).
[22] A. Wallraff *et al.*, Nature (London) **431**, 162 (2004).
[23] L. Frunzio *et al.*, IEEE Trans. Appl. Supercond. **15**, 860 (2005).
[24] D. I. Schuster *et al.* (unpublished).
[25] A. Blais *et al.* (unpublished).